

Living biofouling-resistant membranes as a model for the beneficial use of engineered biofilms

Thammajun L. Wood^{a,b,1}, Rajarshi Guha^{a,1}, Li Tang^a, Michael Geitner^a, Manish Kumar^{a,2}, and Thomas K. Wood^{a,b,c,2}

^aDepartment of Chemical Engineering, Pennsylvania State University, University Park, PA 16802; ^bThe Huck Institutes of the Life Sciences, Pennsylvania State University, University Park, PA 16802; and ^cDepartment of Biochemistry and Molecular Biology, Pennsylvania State University, University Park, PA 16802

Edited by David A. Weitz, Harvard University, Cambridge, MA, and approved April 11, 2016 (received for review November 5, 2015)

Membrane systems are used increasingly for water treatment, recycling water from wastewater, during food processing, and energy production. They thus are a key technology to ensure water, energy, and food sustainability. However, biofouling, the build-up of microbes and their polymeric matrix, clogs these systems and reduces their efficiency. Realizing that a microbial film is inevitable, we engineered a beneficial biofilm that prevents membrane biofouling, limiting its own thickness by sensing the number of its cells that are present via a quorum-sensing circuit. The beneficial biofilm also prevents biofilm formation by deleterious bacteria by secreting nitric oxide, a general biofilm dispersal agent, as demonstrated by both short-term dead-end filtration and long-term cross-flow filtration tests. In addition, the beneficial biofilm was engineered to produce an epoxide hydrolase so that it efficiently removes the environmental pollutant epichlorohydrin. Thus, we have created a living biofouling-resistant membrane system that simultaneously reduces biofouling and provides a platform for biodegradation of persistent organic pollutants.

synthetic circuit | membranes | biofilm dispersal | nitric oxide | biofouling

Access to clean and safe water is essential to human survival (1) and plays an important role in manufacturing, agriculture, and power generation (2). As the demand for fresh water increases worldwide, membrane technologies have emerged as cost-effective approaches to use lower-quality water sources including brackish water, seawater, and recycled wastewater (3). Although microfiltration and ultrafiltration membranes are used to remove particulate matter and microbes from process waters, reverse osmosis (RO) membranes are the leading technology for removing salts and dissolved contaminants from water (4).

Membrane fouling by bacterial biofilms has remained a persistent and unmet challenge for membrane-based water purification systems (5–7). Bacterial biofilms reduce membrane permeability and contaminant rejection and modify membrane module hydrodynamics, resulting in excessive pressure drops both across the membrane (transmembrane pressure drop) and along the membrane axis in membrane modules (axial pressure drop), leading to increased energy consumption (8). In solute-rejecting membranes such as nanofiltration (NF) and RO, biofilms reduce membrane permeability by trapping salt in the biofilm built on the membrane and increasing the osmotic pressure that must be overcome to conduct filtration; this phenomenon is termed “biofilm-enhanced osmotic pressure” (9). Accumulation of solutes and microorganisms on the membrane surface also leads to higher leakage and thus lowers actual solute rejection (9), a major challenge in brackish water treatment and wastewater reuse applications (10, 11). The two most frequently detected deleterious bacteria on RO membranes are *Pseudomonas aeruginosa* and *Sphingomonas wittichii* (12–15).

There are several strategies for controlling membrane biofouling, including adding disinfectants and biocides, adding specific molecules to influence quorum sensing (QS) in biofilms to trigger their dispersal (16–18), and modifying the membrane surface or spacers to reduce biofilm attachment and growth (19–21). However, most current biofouling control techniques either are effective only initially because of the ability of the biofilm to adapt over time to the conditions imposed or need repeated application to control bio-

fouling effectively in the long run; hence, new methods are needed to control persistent biofouling.

Temporal control of mixed-species biofilm formation and dispersal was achieved in a previous study using a synthetic gene circuit based on the autoinducer synthase LasI/response regulator LasR QS system of *P. aeruginosa* by combining it with engineered Hha and engineered biofilm dispersal protein based on c-di-GMP (BdcA) (22). LasI/LasR is one of the best-characterized QS systems in *P. aeruginosa*, and it plays a key role in controlling virulence factor production, swarming motility, biofilm maturation, and the expression of antibiotic efflux pumps (23). Through this QS system, cells monitor their own cell density via exported signals produced by LasI; once a high cell density is reached, the signals diffuse back into the cells and activate genes by binding to the transcription regulator LasR. Previous applications have used the QS signal from one strain to control other strains. However, gene circuits have not been used previously to impose self-regulation, i.e., to control biofilm formation and thickness by the strain producing the QS signal itself.

The final stage of biofilm formation is dispersal, which contributes to survival and biofilm propagation in distant regions (24). Dispersal may be triggered by changes in the environment including nutrient levels, oxygen, pH, and temperature and occurs under favorable and unfavorable conditions to expand the bacterial cellular population (24). Upon these changes in the environment, dispersal is regulated via QS cues such as acylhomoserine lactones and 2-heptyl-3-hydroxy-4-quinolone (24) and by fatty acid signals such as *cis*-2-decenoic acid (25), nitric oxide (NO) (26), and cyclic diguanylate (c-di-GMP) (27). As biofilms disperse, cells degrade

Significance

Biofouling is a significant problem for membrane-based systems because it reduces flow and increases energy consumption. This work shows a previously unreported approach to prevent membrane biofouling by using a beneficial biofilm. The beneficial strain was engineered to have a dispersal “feedback circuit,” based on secretion and uptake of a communication signal, limiting its own biofilm formation by self-monitoring and selective dispersal. The beneficial strain was also engineered to produce nitric oxide, which prevents biofilm formation by harmful bacteria; biofouling by the two most prevalent organisms was shown to be controlled by the beneficial strain. Moreover, the beneficial biofilm was engineered to produce an evolved epoxide hydrolase to enable it to remove the environmental pollutant epichlorohydrin.

Author contributions: T.L.W., R.G., M.K., and T.K.W. designed research; T.L.W., R.G., L.T., and M.G. performed research; T.L.W., R.G., M.K., and T.K.W. analyzed data; and T.L.W., R.G., M.K., and T.K.W. wrote the paper.

The authors declare no conflict of interest.

This article is a PNAS Direct Submission.

Freely available online through the PNAS open access option.

¹T.L.W. and R.G. contributed equally to this work.

²To whom correspondence may be addressed. Email: manish.kumar@psu.edu or tuw14@psu.edu.

This article contains supporting information online at www.pnas.org/lookup/suppl/doi:10.1073/pnas.1521731113/-DCSupplemental.

their extracellular matrix; for example, upon dispersal, *P. aeruginosa* uses endoglycosidase PslG to degrade its primary biofilm exopolysaccharide Psl (28) and also degrades extracellular lipids and proteins of the biofilm matrix (29).

The dispersal signal and secondary messenger c-di-GMP is ubiquitous in Gram-negative bacteria and enhances biofilm formation (30); for example, c-di-GMP increases extracellular polysaccharide production by binding the PelD protein that is a c-di-GMP receptor in *P. aeruginosa* PA14 (31). Thus, biofilm formation and dispersal are controlled by a signal cascade mediated by c-di-GMP levels: High levels promote biofilm formation, and low levels lead to reduced biofilm formation and increased dispersal. NO induces biofilm dispersal by enhancing the activity of phosphodiesterases, resulting in the degradation of c-di-GMP (32). NO is effective in dispersing a variety of different biofilms (26), including *P. aeruginosa* biofilms (32), and NO synthase (NOS) from *Bacillus anthracis* is active in *Escherichia coli* (33). Also, sphingomonad biofilms should be dispersed by NO, because strains such as *S. wittichii* contain 40 diguanylate cyclases and phosphodiesterases (34). Hence, NOS was used in this study to generate NO to disperse deleterious biofilms.

Here we describe a system to reduce the biofouling of water-treatment membranes significantly while degrading an important class of contaminants. Specifically, we engineered a beneficial biofilm of *E. coli* via genetic circuits (i) to limit its biofilm formation, (ii) to prevent biofouling by the two most common biofouling organisms, and (iii) to degrade the model environmental pollutant and water contaminant epichlorohydrin (35–37). To create these beneficial traits, the LasI/LasR QS system of *P. aeruginosa* was used to control the engineered biofilm dispersal protein BdcA of *E. coli* to create the first (to our knowledge) self-controlled biofilm. Additionally, NO was generated in the beneficial biofilm by NOS from *B. anthracis* to prevent biofouling. The effectiveness of this strategy in creating biofouling-resistant membranes was demonstrated using both short-term dead-end filtration tests and long-term cross-flow tests lasting several days under a variety of conditions. We also demonstrate that epichlorohydrin, which passes through the membrane, is degraded by cloning the gene encoding epoxide hydrolase (EH) from *Agrobacterium radiobacter* AD1 into the beneficial biofilm.

Results

Biofilm Formation Is Limited in the Self-Controlled Strain. To form a beneficial biofilm layer on membranes, we desired a protective biofilm that does not attain a large thickness and that prevents the growth of other bacteria so that membrane permeability and salt rejection are maintained and cross-flow pressure drops are minimized. Hence, we devised a genetic circuit in which the bacterium senses its own presence to limit its biofilm formation (Fig. 1A). To do so, we used the LasI/LasR QS system of *P. aeruginosa* (38) to produce the autoinducer molecule *N*-(3-oxo-dodecanoyl)-L-homoserine lactone (3oC12HSL), which accumulates as the cell density increases and induces the formation of a biofilm dispersal protein, BdcA (22), which limits the biofilm quantity and thus thickness of the protective strain. We used the BdcA E50Q variant because it causes sixfold higher levels of biofilm dispersal (39). Specifically, the response regulator LasR is produced continuously and monitors the presence of the QS signal 3oC12HSL produced by LasI; as the 3oC12HSL signal increases because of increasing cell density, additional 3oC12HSL signal is produced as LasR bound to 3oC12HSL activates *lasI*. Increased production of the 3oC12HSL signal activates the dispersal protein BdcA, which leads to dispersal of the beneficial biofilm.

The resulting self-controlled biofilm strain is *E. coli* TG1/pBdcAE50Q-*lasI-lasR* (hereafter the “self-controlled strain”); *E. coli* TG1/pBdcAE50Q-*rfp-lasR* (22), which lacks LasI (hereafter, the “QS signal-negative strain”), was used as a negative control. To demonstrate that the self-controlled biofilm strain can self-regulate its biofilm, both a 96-well plate crystal violet biofilm assay and a confocal microscope biofilm assay were performed. For the 96-well plate assay, the self-controlled biofilm strain had approximately

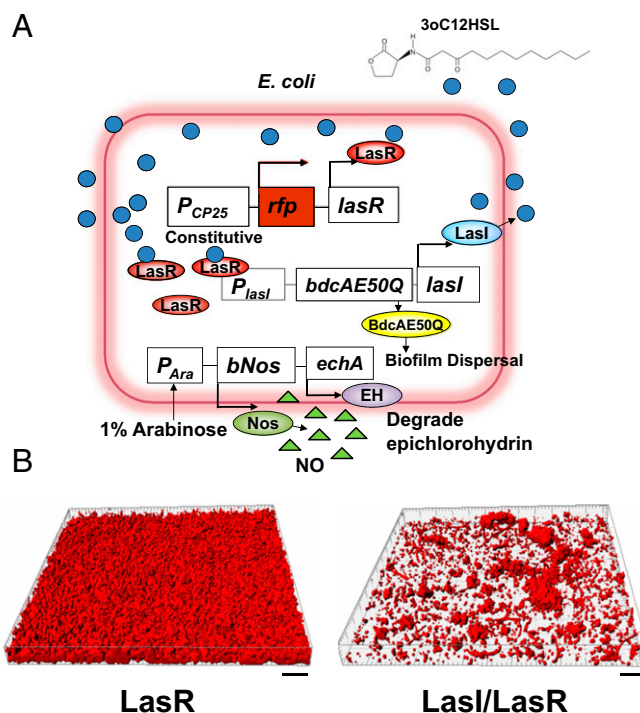


Fig. 1. The self-controlled strain can regulate its own biofilm growth. (A) Gene circuit for the self-controlled biofilm strain. *E. coli* was engineered to limit its own biofilm formation using the LasI/LasR QS module of *P. aeruginosa*. The genes for the LasI protein and the engineered biofilm dispersal protein BdcA E50Q are controlled by the *lasI* promoter. When LasI is produced, it synthesizes the QS signal 3oC12HSL; upon reaching a threshold value based on increasing cell density, the QS signal binds to LasR (which is constitutively produced via the CP25 promoter along with RFP to visualize the cells). The 3oC12HSL+LasR complex activates the *lasI* promoter, which leads to increasing production of dispersal protein BdcA E50Q as cell density increases. The BNos and epoxide hydrolase are induced by adding arabinose. (B) Biofilm formation visualized with confocal microscopy on glass surfaces after 48 h for the QS signal-negative control strain (LasR) that lacks LasI (TG1/pBdcAE50Q-*rfp-lasR*) and the LasI/LasR self-controlled biofilm strain (TG1/pBdcAE50Q-*lasI-lasR*). (Scale bars, 20 μm .) LasR (control) vs. LasI/LasR biofilm values for these figures were $4.2 \mu\text{m}^3/\mu\text{m}^2$ vs. $0.52 \mu\text{m}^3/\mu\text{m}^2$, respectively, for average biomass and $9.11 \mu\text{m}$ vs. $1.18 \mu\text{m}$, respectively, for average thickness.

ninefold less biofilm after 24 h than the QS signal-negative control strain (SI Appendix, Fig. S1). This result was corroborated using confocal microscopy: After 2 d, the self-controlled biofilm was sixfold less than the biofilm of the QS signal-negative control strain (average biomass $0.6 \pm 0.6 \mu\text{m}^3/\mu\text{m}^2$ vs. $3.5 \pm 1 \mu\text{m}^3/\mu\text{m}^2$ and average thickness $1.5 \pm 1 \mu\text{m}$ vs. $7.6 \pm 2 \mu\text{m}$, for the self-controlled and control biofilms, respectively; representative figures are shown in Fig. 1B). Therefore, using the biofilm dispersal protein BdcA under the control of a QS circuit, this gene circuit controlled biofilm formation successfully as a function of cell density.

Membrane Flux Is Higher with the Self-Controlled Biofilm. Biofilms of the self-controlled biofilm strain and the QS signal-negative strain were grown on commercially available NF90 thin film composite polyamide NF membranes. The QS signal-negative strain formed thick and more uniform biofilms over the polyamide NF90 membrane (Fig. 2A and B), whereas the self-controlled strain developed a considerably thinner and more heterogeneous biofilm with ~ 42 -fold lower biomass ($0.2 \pm 0.1 \mu\text{m}^3/\mu\text{m}^2$) than that formed by the control QS signal-negative strain ($8.4 \pm 7 \mu\text{m}^3/\mu\text{m}^2$) (Fig. 2C and SI Appendix, Tables S1 and S2). This result confirms our previous results showing that the QS circuit reduces biofilm formation (Fig. 1B). More importantly, it shows that the synthetic circuit we

assembled regulates its own biofilm amount and thickness on commercial membranes.

Water fluxes through the membrane were measured at different feed salt (NaCl) concentrations to compare the effect of biofouling by the self-controlled strain with that by the QS signal-negative strain. By measuring filtered water flux, known as “permeate flux,” at a series of NaCl concentrations, the resistance of the membrane to water flow can be evaluated. Comparing clean membrane fluxes (incubated with medium) with fouled membrane fluxes (incubated with medium and biomass) provides a measure of biofilm resistance. On the other hand, tracking salt rejection for different biofilms provides an understanding of the extent of salt accumulation (or the degree of concentration polarization) at the membrane surface and its contribution to flux decline. An accounting of the clean membrane resistance and biofilm resistances under various conditions is provided in *SI Appendix, Fig. S2 and Table S3*.

A series of flux experiments for three independent colonies of each strain revealed that application of the self-control synthetic circuit can decrease flux decline caused by uncontrolled fouling by 50% (Fig. 2D). Moreover, when the self-controlled strain was used, NaCl rejection was improved by 11%, indicating lower concentration polarization (*SI Appendix, Table S4*). Overall, by controlling its biofilm formation, the self-controlled biofilm increases operating membrane flux significantly by reducing biofouling.

Deleterious Biofilm Formation Is Reduced and Permeate Flux Is Increased by the Beneficial Biofilm That Produces NO. To create a strain capable of dispersing a wide range of biofilms to limit biofouling on RO membranes, the gene encoding NOS from *Bacillus subtilis* (*bNos*) (33) was added to the self-controlled strain to form a strain that limits its own biofilm formation and also produces NO to disperse deleterious biofilms. This strain, is referred to as “*E. coli* TG1/pBdcAE50Q-*lasI-lasR*/pBNos” (cell schematic shown in Fig. 1A), henceforth “beneficial biofilm strain.” A 96-well plate assay

was performed to confirm that the QS circuit was still active after the addition of pBNos plasmid; the beneficial biofilm strain had sixfold less biofilm after 24 h than the negative control strain (*E. coli* TG1/pBdcAE50Q-*lasI-lasR*/pBad), which lacks NO synthesis (*SI Appendix, Fig. S1*). After 24 h, the beneficial biofilm strain produced $11 \pm 4 \mu\text{M}$ of NO, three- to sixfold higher than the control strain *E. coli* TG1/pBdcAE50Q-*lasI-lasR*/pBad (Fig. 3A).

P. aeruginosa, which is ubiquitous in soil and water, is one of the most prevalent biofouling strains in membrane systems and has been isolated from biofilms on water treatment membranes (12, 13, 15). It is used as a model bacterium for membrane-fouling studies because of its ability to form biofilms and because the genetic basis of its biofilm formation is well studied (40). Sphingomonads are another key biofouling organism in membrane systems; they colonize membrane and spacer surfaces rapidly and cover them with their extracellular polymeric substances (14). Therefore *S. wittichii* (41) also was used in this study as a model bacterium for biofouling.

To demonstrate that the beneficial biofilm strain can inhibit biofilm formation on membranes by deleterious bacteria, the activity of NO against the biofilm formation of *P. aeruginosa* was assayed by tagging the beneficial biofilm with red fluorescent protein (RFP) and *P. aeruginosa* with green fluorescent protein (GFP). Confocal microscopy (Fig. 3 B–E) showed that the beneficial biofilm strain reduced the *P. aeruginosa* biofilm biomass by around 40-fold and reduced the average biofilm thickness by around 100-fold (Fig. 3F) compared with the negative control *E. coli* TG1/pBdcAE50Q-*lasI-lasR*/pBad, which does not produce NO. Critically, in the absence of NO, the *P. aeruginosa* biofilm dominated the *E. coli* control biofilm by forming sporadic patches on the membrane, often where *E. coli* was present [*P. aeruginosa* consortial biofilm (PAO1) and *E. coli* NO⁻ in *SI Appendix, Table S5*], reducing membrane flux by almost 31% after 15 h compared with the self-controlled strain without *P. aeruginosa* (PAO1 and *E. coli* NO⁻ in Fig. 3 G and *E. coli* NO⁻ in *SI Appendix, Fig. S3*). However,

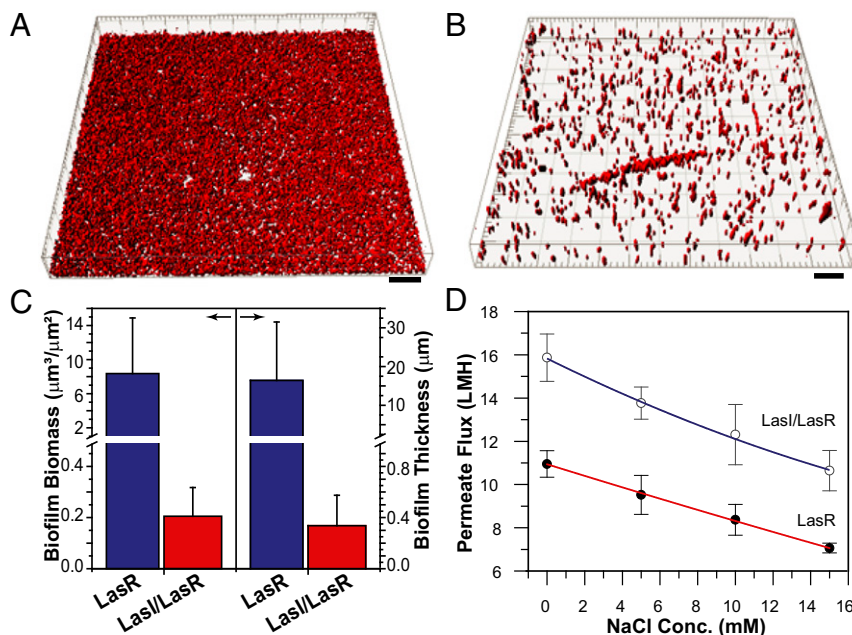


Fig. 2. The self-controlled strain biofilm increases membrane permeate flux. Comparison of growth and resulting permeate fluxes for *E. coli* TG1/pBdcAE50Q-*lasI-lasR* (the self-controlled strain, LasI/LasR) and *E. coli* TG1/pBdcAE50Q-*rfp-lasR* (22), which lacks LasI (the QS signal-negative strain, LasR), on NF90 membranes. (A) Representative image of the uncontrolled biofilm formed for the QS signal-negative strain on membranes after 24 h. Additional images of biofilm are provided in *SI Appendix, Table S1*. (B) Representative image of the biofilm formed by the self-controlled strain on membranes after 24 h. Additional images of biofilm are provided in *SI Appendix, Table S2*. (Scale bars, 20 μm.) (C) Biofilm biomass and average biofilm thickness for the QS signal-negative strain and the self-controlled strain. (D) Comparisons of permeate flux through membranes with the self-controlled strain and the QS signal-negative control strain. All values are averages of three independent colonies ($n = 3$), and the error bars are SD from six samples.

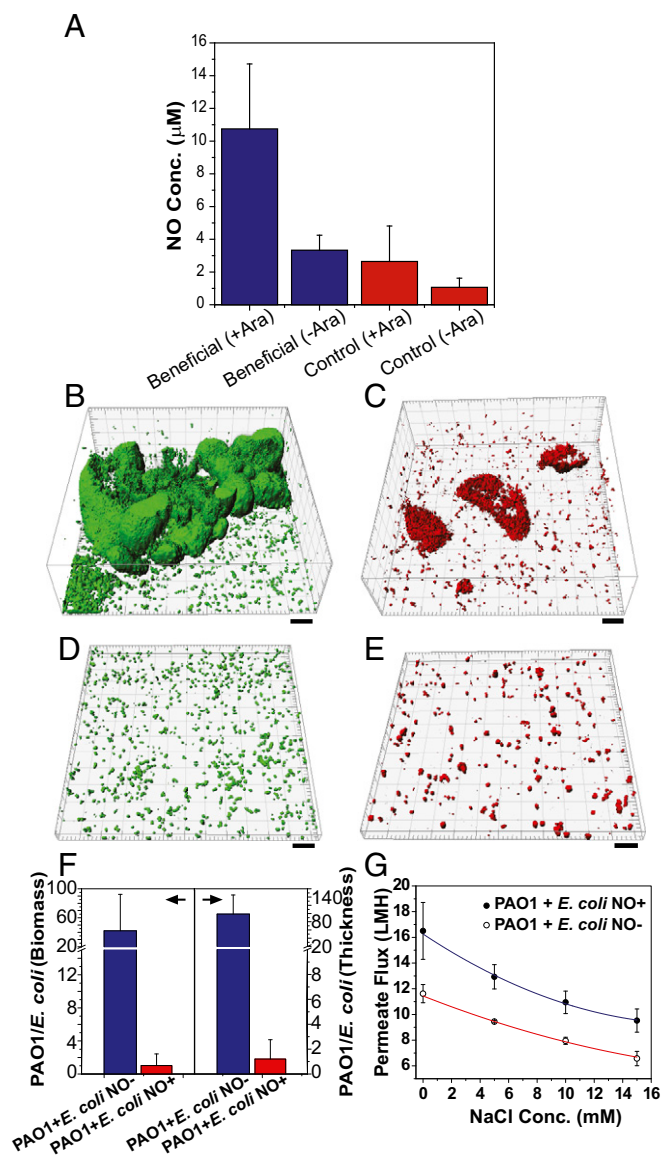


Fig. 3. The NO-producing beneficial biofilm decreases *P. aeruginosa* biofilm formation on membranes. (A) NO production by the beneficial biofilm strain (*E. coli* TG1/pBdcAE50Q-*lasI-lasR*/pBNos) after 24 h in M9G medium with 15 mM arginine (substrate for NOS) compared with the control strain (*E. coli* TG1/pBdcAE50Q-*lasI-lasR*/pBad). Arabinose induces the *bNos* gene. Confocal microscopy was used to discern the biofilm formation of the *P. aeruginosa* and the *E. coli* beneficial biofilm consortium developed on the RO membrane after 48 h. The biofilm formation by each bacterium in the consortium is shown separately. (B and C) *P. aeruginosa* consortial biofilm (PAO1) (B) and consortial biofilm of the *E. coli* control strain (*E. coli* TG1/pBdcAE50Q-*lasI-lasR*/pBad) that does not produce NO (*E. coli* NO⁻) (C). (D and E) Consortium of the *P. aeruginosa* biofilm (D) and the beneficial biofilm strain (*E. coli* TG1/pBdcAE50Q-*lasI-lasR*/pBNos, *E. coli* NO⁺) (E). (Scale bars, 20 μm.) Representative images are shown; additional images are shown in *SI Appendix, Tables S5 and S6*. (F) COMSTAT analysis of the ratio of the consortia biofilm biomass and ratio of the average thickness. The error bars represent SDs from a sample size of 15. (G) Membrane flux measurements with *P. aeruginosa* (PAO1)/*E. coli* biofilm consortia on NF90 membranes. The error bars are SDs from three independent experiments for each type of consortial challenge, i.e., PAO1/*E. coli* NO⁻ and PAO1/*E. coli* NO⁺.

production of NO by the beneficial biofilm strain reduced biofouling by reducing the biofilm of the deleterious species (PAO1 and *E. coli* NO⁺ in Fig. 3G). Without NO, the control biofilm generated 165% more resistance to flux because of *P. aeruginosa* infiltration into the

biofilm (*SI Appendix, Table S3*). Thus, the control consortial biofilm generated an additional resistance that approximately doubled the clean membrane resistance, whereas the beneficial biofilm essentially negated this increase. The beneficial biofilm produced permeate flux similar to that of the self-controlled strain (compare *LasI/LasR* in Fig. 2D with *E. coli* NO⁺ in *SI Appendix, Fig. S3*), so the production of NO by the beneficial strain did not affect permeate flux. As a positive control for NO dispersal of *P. aeruginosa*, sodium nitroprusside (SNP) was used to generate NO, which dispersed the *P. aeruginosa* biofilm in 96-well plates; at 5 μM SNP, normalized *P. aeruginosa* biofilm was reduced by 80% (*SI Appendix, Fig. S4*). Therefore, by controlling the formation of the deleterious biofilm strain by the production of NO, the self-controlled biofilm increased membrane operating flux.

We also investigated the ability of the beneficial biofilm to inhibit the biofilm of the other prominent biofouling organism, *S. wittichii*. *S. wittichii* produced less biofilm than *P. aeruginosa* under all conditions tested (*SI Appendix, Fig. S5*). On membranes with consortia, without the presence of NO, the control strain *E. coli* TG1/pBdcAE50Q-*lasI-lasR*/pBad could not prevent *S. wittichii* biofilm formation after 2 d, as evident from the larger total biofilm biomass found on the membrane (Fig. 4A) relative to the *E. coli* control strain portion of the consortial biofilm (Fig. 4B); in fact, most of the consortial biofilm was that of *S. wittichii*. In contrast, in the presence of NO produced by the beneficial biofilm strain (*E. coli* TG1/pBdcAE50Q-*lasI-lasR*/pBNos), total biofilm formation (Fig. 4C) was reduced by more than an order of magnitude (Fig. 4E). Because the biofilm biomass of the portion of the consortium that is the beneficial strain (Fig. 4D) is roughly the same as the total biofilm (Fig. 4C), the *S. wittichii* biofilm was almost completely eliminated when NO was produced by the beneficial biofilm strain. Therefore, our beneficial strain provides a general solution for preventing biofouling because it reduces biofilm formation by both *P. aeruginosa* and *S. wittichii*. Note that, unlike the consortial biofilm experiments with *P. aeruginosa*, in which the pseudomonad was tagged with GFP, we determined the *S. wittichii* biofilm levels by subtracting the *E. coli* biofilm levels (determined by RFP levels) from the total biofilm that was determined by staining both strains with SYTO9 (green).

We also conducted long-term cross-flow filtration challenge tests to determine the robustness of our approach under the shear and pressure conditions typically seen in spiral-wound membrane systems operating at plant scales. We conducted these tests for 2–5 d, leading to substantial declines in productivity, reaching over 50%, with a well-validated cross-flow system (Osmonics SEPA Cell) with Dow NF90 membranes and a computerized control system built to allow operation at constant pressure. In all experiments, the membranes were first conditioned with either the control strain (the self-controlled strain with no NO release capabilities, *E. coli* NO⁻, TG1/pBdcAE50Q-*lasI-lasR*/pBad) or the beneficial strain (the self-controlled strain with NO release capabilities, *E. coli* NO⁺, TG1/pBdcAE50Q-*lasI-lasR*/pBNos) for 24 h in cross-flow mode but with minimal permeation by maintaining a transmembrane pressure of 40 psi, and then the pressure was increased to 200 psi and permeate measured. The system conditioned with control biofilms (*E. coli* NO⁻) showed a rapid flux decline in 4,000 min (~3 d) to ~55% of initial flux, whereas the beneficial biofilm restricted the flux decline to ~34%, a decrease of ~40% (Fig. 5). Critically, the beneficial biofilm-enhanced membranes could be run longer, for ~4 d, under challenge conditions without the flux decline reaching 50% (*SI Appendix, Fig. S6*). In these experiments the conditioning biofilms were started with an initial *E. coli* turbidity at 600 nm of 0.01 in the system feed and were challenged with *P. aeruginosa* PAO1 at an initial turbidity of 0.002 in the system feed. Another set of experiments was conducted with higher microbial loads (initial conditioning films with *E. coli* at a turbidity of 0.05 and *P. aeruginosa* PAO1 at a turbidity of 0.01) and led to similar differences in flux decline but over a shorter time scale (~24 h of challenge) (*SI Appendix, Fig. S7*).

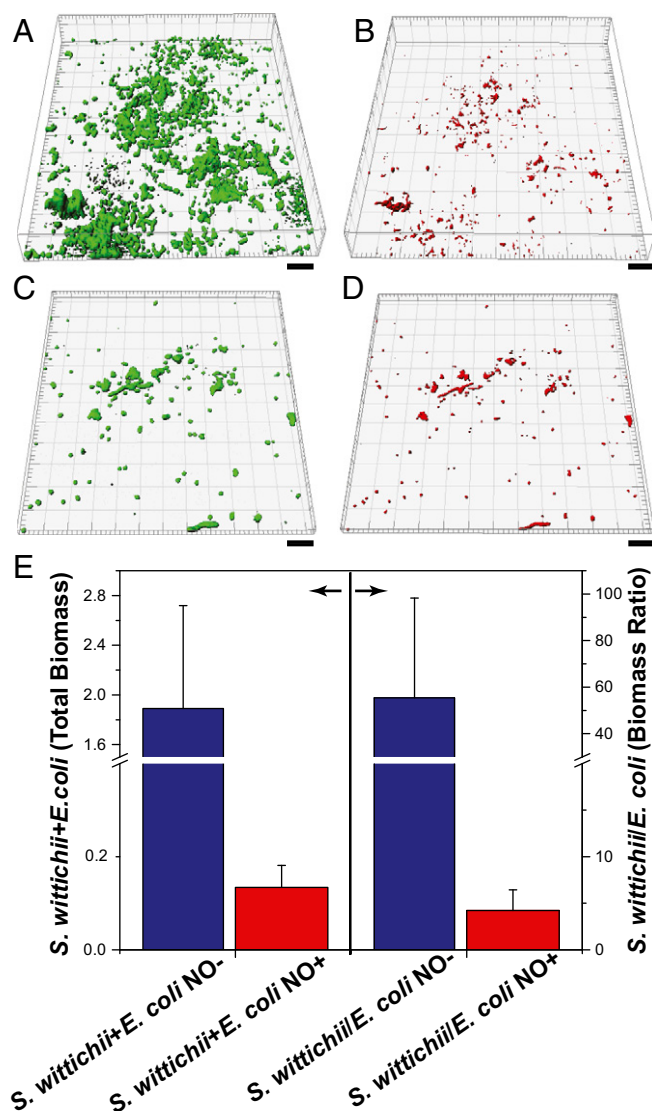


Fig. 4. The NO-producing beneficial biofilm decreases *S. wittichii* biofilm formation on membranes. (A) Total biofilm of the consortium of *S. wittichii* with the control (*E. coli* TG1/pBdcAE50Q-*lasI-lasR*/pBad, *E. coli* NO⁻) after 48-h challenge at 30 °C in M9G medium supplemented with 15 mM arginine and 1.6% arabinose. The confocal images were taken after SYTO9 staining to observe total biofilm on the membranes. (B) Consortial biofilm of the RFP-tagged control strain which did not produce NO (*E. coli* NO⁻). (C) Total biofilm of the consortium of *S. wittichii* and the beneficial biofilm strain which produces NO (*E. coli* TG1/pBdcAE50Q-*lasI-lasR*/pBNos, *E. coli* NO⁺). (D) Consortial biofilm of the RFP-tagged, NO-producing, beneficial biofilm strain. (Scale bars, 20 μm.) Representative images are shown; additional images are shown in *SI Appendix, Tables S8 and S9*. (E) COMSTAT analysis of *S. wittichii* and *E. coli* consortial biofilm biomass (expressed in cubic micrometers per square micrometer) and the ratio of *S. wittichii* biomass to *E. coli* biomass. The error bars represent SDs from a sample size of six. *E. coli* biomass (RFP-tagged) was subtracted from the total biomass (stained with SYTO9) to determine the *S. wittichii* biomass.

Biofilm analysis of the membranes subjected to the long-term cross-flow (3–4 d) tests corroborated the permeate flux results, in that an order of magnitude less colonization of the membranes by the challenge organisms (*P. aeruginosa* PAO1) was seen when the membranes were conditioned by the beneficial biofilm (*E. coli* NO⁺) than when membranes were conditioned by the control biofilm (*E. coli* NO⁻) (Fig. 5). The total biomass for the beneficial biofilm-conditioned membranes challenged by *P. aeruginosa* PAO1 was limited to 0.017 (± 0.001) μm³/μm², whereas it was 0.35 (± 0.02) μm³/μm²

for the membranes conditioned by control biofilms. Because both the control and beneficial biofilms were based on the self-controlled LasI/LasR system, the overall biofilm formation was limited, as expected. The biomass value of the control strain alone was ~0.10 μm³/μm² (i.e., the difference between the total biomass and the *P. aeruginosa* PAO1 biomass) at the end of ~4 d, similar to that seen after 1 d for the batch experiments (~0.20 μm³/μm²) (Fig. 2), indicating the self-controlled strain was maintained.

Epichlorohydrin Degradation by the Beneficial Biofilm. Epichlorohydrin is a common precursor for synthesizing glycerins, epoxy resins, elastomers, pesticides, textiles, membranes, paper, and pharmaceuticals (35); it harms the skin, liver, kidneys, and central nervous system and is a potential carcinogen (42). Epichlorohydrin is recognized as a water contaminant and has a concentration limit of zero in water supplies (36, 37). Epichlorohydrin can be degraded by the EH from *A. radiobacter* AD1 (43), and engineered variants of EH (F108L/I219L/C248I) enhance epichlorohydrin degradation sixfold (44); hence, the engineered EH from this organism (44) was used in this study so the beneficial biofilm could simultaneously perform bioremediation and prevent biofouling.

Epichlorohydrin, as a small hydrophobic compound, passes through the membrane used in this study (*SI Appendix, Fig. S8*). As a planktonic culture, the beneficial strain that produces EH from *echA* (*E. coli* TG1/pBdcAE50Q-*lasI-lasR*/pBNos-*echA*) degraded epichlorohydrin at a rate of 3.7 ± 0.4 nmol·min⁻¹·mg⁻¹ of protein (*SI Appendix, Fig. S9*), but there was no epichlorohydrin degradation in the control strain that lacks EH (*E. coli* TG1/pBdcAE50Q-*lasI-lasR*/pBNos). Furthermore, when grown on the NF90 membrane, the beneficial biofilm that produces EH degraded epichlorohydrin by more than 39 ± 4% in single-pass batch filtration (Fig. 6 and *SI Appendix, Fig. S10*). Therefore, the beneficial biofilm that produces EH is capable of degrading the environmental pollutant epichlorohydrin while controlling its own biofilm formation and limiting the biofilm formation of deleterious strains.

Discussion

We have demonstrated a previously unreported approach as a proof of concept and as an industry-relevant system for combating biofouling in membrane systems by using the feature of biofilms that makes them a challenge in many systems—their persistence—in a beneficial manner. At the core of this work is a QS circuit we engineered to create a beneficial biofilm that effectively limits its own biofilm formation. We also produced the biofilm-dispersing agent NO in the beneficial strain and effectively limited the biofilm formation of deleterious bacteria *P. aeruginosa* and *S. wittichii*; both organisms have been demonstrated to be important fouling agents for membranes. We further developed the biofilm into a platform for treating refractory pollutants that escape or are modified through the upstream treatment process and can even pass through RO membranes. Currently micropollutants that pass through NF and RO membranes, such as *N*-nitrosodimethylamine (45) and 1,4-dioxane (46), must be treated using even more advanced techniques such as high-intensity UV radiation (47).

To develop the approach presented further, the plasmid-based systems shown to work here should be stabilized by integrating the required functional elements into the chromosome, thereby limiting the transfer of these genetic elements to other microorganisms. In addition, proven conditional suicide systems may be added that would prevent the beneficial biofilm strain from propagating should it be released (48); however, the evolutionary pressure would be to lose the biofilm self-control circuit, because biofilms are used by nearly all bacteria to increase fitness. Also, our system needs to be tested further for its long-term effectiveness against more complex environmental samples, recognizing that each environmental system may require a different beneficial strain.

We designed the membrane experiments to demonstrate the effectiveness of the beneficial biofilm while carefully considering and balancing actual membrane system operation and the need to

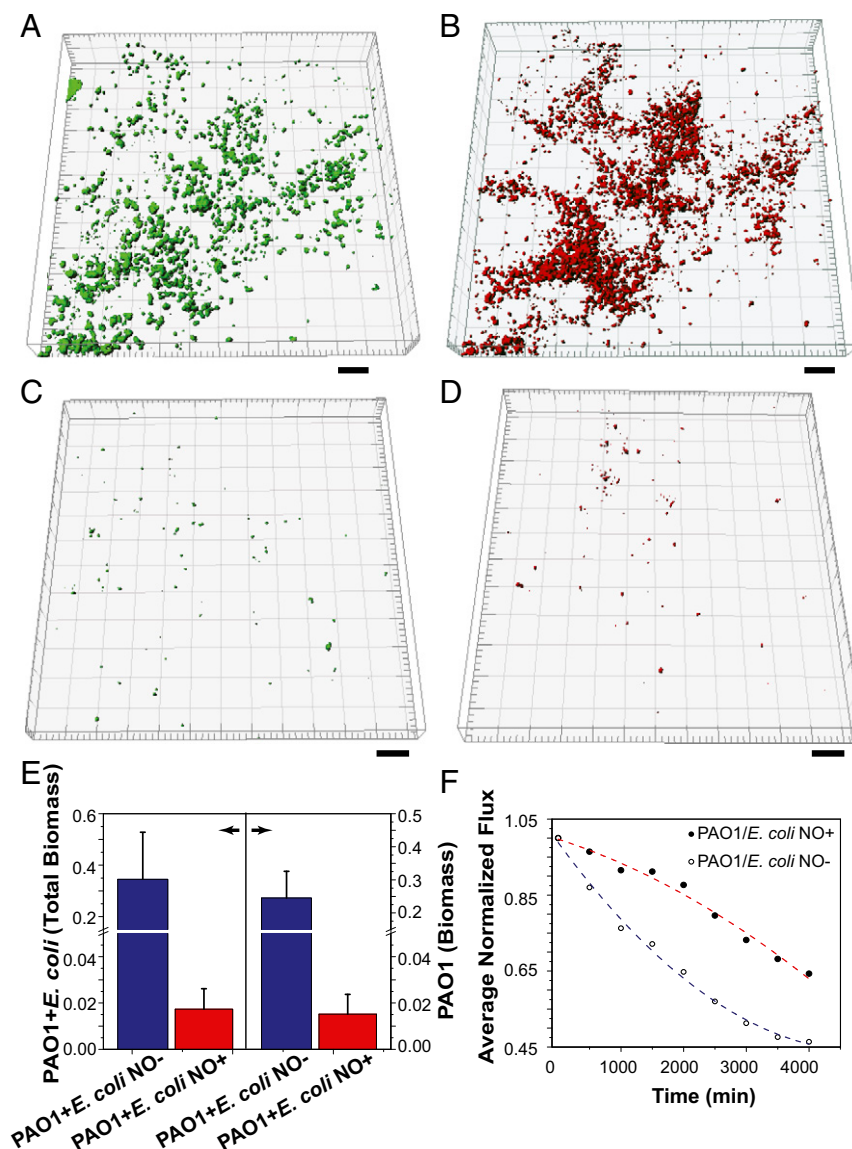


Fig. 5. The beneficial biofilm reduces the formation of *P. aeruginosa* PAO1 biofilm on membranes and mitigates flux decline under cross-flow conditions. (A) Deconvoluted *P. aeruginosa* PAO1 consortial biofilm on an NF90 membrane. (B) Deconvoluted *E. coli* control strain (TG1/pBdcAE50Q-*lasI-lasR*/pBad) that does not produce NO (*E. coli* NO⁻) consortial biofilm on an NF90 at the same position as A. (C and D) Deconvoluted consortium of the *P. aeruginosa* PAO1 biofilm (C) and the beneficial biofilm strain (*E. coli* TG1/pBdcAE50Q-*lasI-lasR*/pBnos, *E. coli* NO⁺) (D) under hydrodynamic conditions similar to those in A and B. (Scale bars, 20 μ m.) Representative images are shown; additional images are in *SI Appendix, Tables S10 and S11*. (E) COMSTAT analysis of consortia biofilm biomass and *P. aeruginosa* PAO1 biomass is expressed in cubic micrometers per square micrometer. The error bars represent SDs from a sample size of six. (F) Average normalized flux profile measured at \sim 200 psi applied pressure under cross-flow conditions with the *P. aeruginosa* (PAO1)/*E. coli* biofilm consortia on NF90 membranes.

obtain reproducible data. Hence, the development of the beneficial biofilm forming the conditioning film on the membrane was conducted both with and without shear, but in all cases at low pressures so no filtration occurred. In full-scale plants, this approach can be implemented by using the cleaning setup to flow cultures through the system in recirculation mode without filtration to build the beneficial biofilm. Such operation in the flushing mode is common during chemical cleaning of membrane modules.

Additionally, the flux measurements were conducted both under filtration conditions in a dead-end mode with the use of a stirred cell that simulates the shear that is seen in cross-flow membrane systems (49) and is a widely used technique for rapid evaluation of fouling trends (50) and in the cross-flow filtration mode under NF/RO practice-relevant conditions. The challenge experiments with *P. aeruginosa* and *S. wittichii* were conducted initially without

shearing and filtration (Figs. 3 and 4) to provide the most conservative estimate of the efficacy of the beneficial biofilms in preventing colonization by these challenge strains (51). We also evaluated the beneficial biofilm by challenging it with *P. aeruginosa* under shear stress using industrially relevant cross-flow and pressure conditions and found that the beneficial biofilm maintained an order of magnitude less biofilm biomass than the control strain (Fig. 5A–E). This result was reflected in \sim 30–40% less flux decline with the beneficial strain than with the control strain under similar hydrodynamic and temporal conditions (Fig. 5F). Therefore, the beneficial strain has been demonstrated to be effective in minimizing biofilm, not only in dead-end batch systems but also under high-pressure and shear-dominated cross-flow conditions used in large-scale applications.

Possible additional industrial settings for the use of the beneficial biofilm include cooling towers, water distribution systems, and

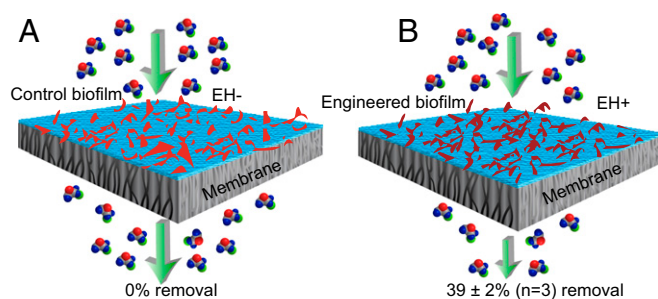


Fig. 6. The beneficial biofilm degrades the micropollutant epichlorohydrin that passes through the membrane. Epichlorohydrin removal was tested using biofilms of *E. coli* [TG1/pBdcAE50Q-*lasI-lasR*/pBNos (EH⁻) and *E. coli* TG1/pBdcAE50Q-*lasI-lasR*/pBNos-*echA* (EH⁺)] developed in 24 h on NF90 membranes in M9G medium with 15 mM arginine and 1.6% arabinose. The control biofilm was challenged with 10 mM epichlorohydrin in 5 mM NaCl feed solution (pH ~9.0). Epichlorohydrin adsorption to the cellular biomass was subtracted from the total removal amount to determine the actual enzymatic removal levels shown here (SI Appendix, Fig. S10). (A) No enzymatic removal was observed with the control biofilm of *E. coli* TG1/pBdcAE50Q-*lasI-lasR*/pBNos (EH⁻) on NF90 membranes. (B) Removal of epichlorohydrin by beneficial biofilm (*E. coli* TG1/pBdcAE50Q-*lasI-lasR*/pBNos-*echA* or EH⁺) was 39% at 30 min after the filtration began under similar process and feed conditions. The error values are SD for three independent colonies.

in-building HVAC systems [implicated in Legionnaires' disease (52, 53)]. The approach proposed also can be extended to other membrane technologies such as membrane bioreactors and forward osmosis for contaminant degradation and biofouling prevention with proper controls on engineered biofilm proliferation.

Beyond water treatment, biomedical applications that would rely on limiting biofilm formation could include biofilm prevention in medical catheters (54), biomedical implants (55), and perhaps even biofilm-related human diseases (56) such as cystic fibrosis (57), endocarditis (58), dental plaque (59), and chronic rhinosinusitis (60). The use of beneficial biofilms to combat biofilm-related diseases could reduce the use of antibiotics and help combat the rise of antibiotic resistance. Treatment of antibiotic-resistant *Helicobacter pylori* infection is relevant in this context (61), because the first-line antibiotics are proving increasingly ineffective against *H. pylori* biofilms (62); the beneficial biofilm, after suitable modifications, possibly could be used as an alternative treatment strategy. Overall, the general scheme we developed has the potential for combating many problems that arise because of the uncontrolled proliferation of bacteria in biofilms.

Methods

Bacterial Strains and Culture Conditions. All strains and plasmids used in this study are summarized in Table 1. All strains were grown in lysogeny broth (LB) (63) or minimal medium with 0.4% glucose (M9G) (64) at 37 °C. Chloramphenicol (Cm) (300 µg/mL) was used to maintain pCA24N-based plasmids in *E. coli*; carbenicillin (Cb) (250 µg/mL) was used to maintain pBad in *E. coli* and also was used to maintain pMRP9-1 in *P. aeruginosa* PAO1; pMRP9-1 allowed *P. aeruginosa* to be tagged with GFP. During coculture with *E. coli*, *P. aeruginosa* was not affected by the Cm (300 µg/mL) because it is naturally resistant to this antibiotic. *S. wittichii* RW1 was obtained from Sharon L. Walker, University of California, Riverside, CA, and was grown in M9G nutrient medium containing peptone (5 g/L) and beef extract (3 g/L) or in LB at 30 °C.

Plasmid Construction. Plasmid pBdcA E50Q-*lasI-lasR* contains *bdcAE50Q* (39) and *lasI* under the control of *lasI* promoter and *rfp* and *lasR* under the control of the constitutive CP25 promoter. *lasI* was amplified from pHha13D6-*gfp-lasI* (22) using the *lasI*-*Sall* forward and *lasI*-*HindIII* reverse primers (SI Appendix, Table S7) and was cloned into pBdcAE50Q (22) at the *Sall* and *HindIII* restriction sites to form pBdcAE50Q-*lasI*. The constitutive promoter CP25, *rfp*, and *lasR* fragment was obtained by digesting the pBdcAE50Q-*rfp-lasR* plasmid (22) with *BspI* and was inserted into the pBdcAE50Q-*lasI* plasmid at the *BspI* site downstream of the *lasI* gene to form pBdcAE50Q-*lasI-lasR*.

To construct the pBNos-*echA* plasmid, the *echA* gene was amplified by PCR using pBSKan (EH, F108L1/219L/C248I) (44) as the template with the EH *HindIII* forward and EH *Sall* reverse primers (SI Appendix, Table S7). The PCR products

were double digested with *HindIII*-HF and *Sall*-HF and ligated into pBNos (33), yielding pBNos-*echA*.

All plasmids were verified by DNA sequencing. The oligonucleotides were synthesized by Integrated DNA Technologies.

Biofilm Formation Assay Using Crystal Violet. Biofilm formation was assayed in 96-well polystyrene plates using 0.1% crystal violet staining as described previously (65) with some modifications. Diluted overnight cultures at an initial turbidity at 600 nm of 0.05 were inoculated into 96-well plates with M9G with appropriate antibiotics, and the bacteria were cultured for 24 h at 37 °C without shaking. SNP (Sigma-Aldrich) was used for the *P. aeruginosa* biofilm dispersal control. After the crystal violet was added to each well, the wells were rinsed and dried, and ethanol was added to dissolve the crystal violet. The total biofilm formation samples were measured at 540 nm, and cell growth was measured at 620 nm. Biofilm formation was normalized by the bacterial growth to reduce any growth effect. At least three independent cultures were used for each strain.

Biofilm Formation Assay Using Confocal Microscopy. The overnight cultures were diluted to an initial turbidity at 600 nm of 0.05 and were inoculated into M9G in glass-bottomed dishes (catalog no. 150680; Nunc, Thermo Scientific) for 24 h at 37 °C without shaking. Fresh M9G medium (1 mL) was added to the dishes, and they were incubated for another 24 h at 37 °C. For the biofilm experiments with *P. aeruginosa*, diluted overnight cultures of *E. coli* (turbidity at 600 nm of 0.01) were inoculated into M9G in glass-bottomed dishes for 24 h at 37 °C without shaking. Overnight cultures of *P. aeruginosa* were added to the dishes at an initial turbidity at 600 nm of 0.1, and 15 mM of arginine and 1% arabinose were added to the culture. The dishes were incubated for another 24 h at 37 °C.

Confocal microscopy images were taken using a 63×/1.4 oil objective lens (HCX PL APO CS 63.0 × 1.4 OIL UV) with a TCS SP5 scanning confocal laser microscope (Leica Microsystems), and images were obtained using an argon laser with emission set between ~500 and 540 nm in one photomultiplier tube (green channel) and emission set between ~550 and 650 nm in the other photomultiplier tube (red channel). A double dichoric lens was used to filter emitted light to visualize RFP (*E. coli*), and a triple dichoric lens was used to filter emitted light to observe both RFP (*E. coli*) and GFP (*P. aeruginosa*). For consortia of *S. wittichii* and *E. coli*, membrane samples were incubated with 5 mL 5 µM SYTO 9 in 0.85% NaCl for 1 h under light-insulated conditions to stain the total biofilm from both *S. wittichii* and *E. coli* and were washed with 0.85% sterile NaCl solution to remove excess dye. The samples were analyzed using the same procedure, except that the red channel emission was collected between ~560 and 650 nm (for RFP-tagged *E. coli*) to minimize interference from the green channel. The *S. wittichii* biofilm cells were determined by subtracting the red *E. coli* biofilm signal from the total green signal. Using the confocal z-stack images, 3D reconstruction of the biofilm architecture was performed using IMARIS software (Bitplane Inc.). Biomass was obtained using COMSTAT image-processing software (66). At least three different areas were observed, and average biomass was reported. At least three independent cultures were tested in this manner, and representative images are shown.

NO Assay. The final products of NO produced in vivo are nitrite and nitrate; thus, the sum of the nitrite and nitrate concentrations is directly correlated to the level of NO production (33). Nitrate and nitrite concentrations were measured using a nitrate/nitrite colorimetric assay kit (Cayman Chemicals). Diluted overnight cultures at an initial turbidity at 600 nm of 0.05 were inoculated into M9G for 48 h at 37 °C. Arginine (15 mM) was added as the substrate, and 1% arabinose was added to induce NO production. At least three independent cultures were tested.

EH Assay. A chromogenic reaction of epoxide epichlorohydrin with 4-nitrobenzylpyridine was used to measure the activity of EH (67) using planktonic cells. The assay was performed in 1.5-mL microcentrifuge tubes as described previously (44). Diluted overnight cultures at an initial turbidity at 600 nm of 0.05 were inoculated in LB with 1% arabinose at 37 °C. The culture (100 µL) at an initial turbidity at 600 nm of 1 was contacted with 400 µL of 5 mM epichlorohydrin in Tris EDTA buffer (pH 9.0) at 37 °C; then 250 µL of 4-nitrobenzylpyridine [100 mM in 80% (vol/vol) ethylene glycol and 20% (vol/vol) acetone] was added. After the samples were heated at 80 °C for 10 min, 250 µL of 50% trimethylamine (in acetone) was added. The samples were measured at 520 nm. At least three independent cultures were tested. The protein content of *E. coli* TG1 (68) (0.22 mg of protein·mL⁻¹·OD⁻¹) was used to calculate the epichlorohydrin degradation rate.

Dead-End Filtration Membrane Biofilms. Biofilms were grown on membranes for 24 h in M9G in a VWR gravity convection incubator. The membrane used

Table 1. Bacterial strains and plasmids used in this study

Strain or plasmid	Description	Source
Strains		
<i>E. coli</i> TG1	<i>supE thi-1 Δ(lac-proAB) Δ(mcrB-hsdSM)5, (r_K⁻ m_K⁻)</i> F' [traD36 proAB ⁺ lacI ^q lacZΔM15]	(64)
<i>P. aeruginosa</i> PAO1	Wild-type	(70)
Plasmids		
pHha13D6- <i>gfp-lasl</i>	Cm ^R ; lacI ^q , pCA24N P _{T5-lac} :: <i>hha13D6</i> ⁺	(22)
pBdcAE50Q	Cm ^R ; lacI ^q , pCA24N P _{lasI} :: <i>bdcAE50Q</i> ⁺	(22)
pBdcAE50Q- <i>rfp-lasR</i>	Cm ^R ; lacI ^q , pCA24N P _{lasI} :: <i>bdcAE50Q</i> ⁺ P _{CP25} :: <i>rfp</i> ⁺ - <i>lasR</i> ⁺	(22)
pBdcAE50Q- <i>lasI-lasR</i>	Cm ^R ; lacI ^q , pCA24N P _{lasI} :: <i>bdcAE50Q</i> ⁺ - <i>lasI</i> ⁺ P _{CP25} :: <i>rfp</i> ⁺ - <i>lasR</i> ⁺	This study
pBNos	Cb ^R ; pBad P _{Ara} :: <i>nos</i> ⁺	(33)
pBNos- <i>echA</i>	Cb ^R ; pBad P _{Ara} :: <i>nos</i> ⁺ <i>echA</i> (F108L/I219L/C248I) ⁺	This study
pBad/Myc-HisB	Cb ^R ; <i>araC</i>	Invitrogen
pMRP9-1	Cb ^R ; pUCP18 carrying a gene encoding enhanced GFP	(71)

Cb^R, carbenicillin resistance; Cm^R, chloramphenicol resistance.

was the commercially available DOW NF90 thin film composite polyamide type. An Advantec MFS UHP-76 stirred cell with an effective membrane area of 35.3 cm² was used for growing biofilms on membranes and for conducting permeability tests. A flat sheet of the NF90 membrane was placed under the O-ring and above the spacer of the stirred cell. The inner volume (450 mL) of the stirred cell was sterilized with 95% ethanol, and cells were adjusted to a turbidity at 600 nm of 0.5 in M9G medium. The cells were added to the stirred cell to a total liquid volume of 300 mL and were grown without stirring for 24 h to form the biofilm. Small pieces of the membranes (~5 × 5 mm) were used for confocal laser-scanning microscopy.

Dead-End Filtration Consortial Biofilms. To challenge the beneficial biofilm with *P. aeruginosa* PAO1/pMRP9-1 (GFP tagged) and to ascertain the dispersal activity of the beneficial strain, both the NO⁻ control strain, *E. coli* TG1/pBdcAE50Q-*lasI-lasR*/pBad, and the *E. coli* NO⁺ beneficial strain, *E. coli* TG1/pBdcAE50Q-*lasI-lasR*/pBNos, (both RFP tagged) were grown as biofilms on NF90 membranes for 24 h as described above. The medium was discarded and was replaced with fresh M9G medium (300 mL) containing 15 mM L-arginine (substrate for NO synthase) and 1.6% L-arabinose inducer for *bNos*. An overnight culture of *P. aeruginosa* in LB with 1.6% arabinose and 15 mM of arginine was added to each stirred cell to make an initial turbidity at 600 nm of 0.1. The stirred cells were incubated for 24 h. Small sections of the membranes from different regions were imaged for biofilms under confocal microscopy using combined green and red fluorescence lasers. At least 15 different membrane biofilm samples, spanning three independent cultures, were analyzed to determine average biofilm thickness and biomass.

The beneficial biofilm was grown under similar conditions for challenge with *S. wittichii*. After 24 h of growth of the *E. coli* NO⁺ beneficial strain (*E. coli* TG1/pBdcAE50Q-*lasI-lasR*/pBNos) or the NO⁻ control strain (*E. coli* TG1/pBdcAE50Q-*lasI-lasR*/pBad), the medium was removed, and the stirred cell was washed with M9G without any antibiotics. An overnight culture of *S. wittichii* in LB with 1.6% arabinose and 15 mM of arginine was added to each stirred cell to make an initial turbidity at 600 nm of 0.5 in M9G medium without antibiotics. The stirred cells were incubated for 48 h at 30 °C, the medium was removed, and the membrane samples were stained with SYTO9.

Dead-End Filtration Membrane Flux Assays. All flux measurements were conducted under filtration conditions in a stirred cell that simulates the shear seen in cross-flow membrane systems; this technique is widely used for rapid evaluation of fouling trends (49, 69) and has been used for the development of fouling indices. Flux experiments were performed immediately following biofilm growth using 0, 5, 10, and 15 mM NaCl. After the medium was removed, the stirred cell was washed three times with 15 mM NaCl, and the stirrer and sample-withdrawal tubes were loaded into the cells. Simultaneously, solutions of 25% feed NaCl concentrations were loaded into the 1-L Amicon reservoir (EMD Millipore). In this way, any variation of feed concentration during the flux experiment in the dead-end filtration mode was minimized. The reservoir NaCl concentrations were 0, 1.25, 2.5, and 3.75 mM. Thereafter, the reservoir and the stirred cell were pressurized to 50 psi using N₂, and the stirring speed was maintained at 400 rpm. Permeate water weight was collected every 30 s using an automated A&D FX-300i balance and analyzed using WinCT RS Weight software, v. 3.00. The experiments were continued for 20–30 min for each feed concentration. Conductivities of permeate and feed were measured using an

Orion VERSA STAR conductivity meter (model VSTAR 50) from Thermo Scientific. The measured flux in grams per minute was converted into liters per square meter per hour for comparisons of membrane performance.

Long-Term Cross-Flow Filtration Biofilm Challenge Experiments. Biofilm development under cross-flow conditions was performed according to Herzberg and Elimelech (9) with some modifications. A 0.5% bleach solution was circulated through the cross-flow RO system built around an Osmonics SEPA cell (Sterilitech) for 2 h in recirculation mode to disinfect the system. Following disinfection, deionized (DI) water was introduced in flushing mode to rinse the system for 10 min, and then trace organic matter was removed with 5 mM EDTA at pH ~11 (1 mM NaOH) under recirculation mode for 30 min. The unit was rinsed again with DI water for 30 min in flushing mode, and 95% ethanol was recirculated through the system for 1 h for further sterilization. Autoclaved DI water was introduced to flush the system of residual ethanol. An ethanol-sterilized and autoclaved water-washed NF90 membrane was loaded in the system along with a feed spacer (as indicated), and membrane compaction was performed overnight with autoclaved DI water with the temperature adjusted to 27 °C at 200 psi. Four liters of M9G medium was introduced with 300 μg/mL Cm and 250 μg/mL Cb without arginine/arabinose, and the membrane was conditioned for 4 h at 27 °C at 200 psi. Centrifuged (3,750 × *g* for 10 min at 4 °C) *E. coli* NO⁻ or *E. coli* NO⁺ cells from overnight cultures were added to the 4 L of M9G medium to an initial turbidity at 600 nm of 0.01 or 0.05. The *E. coli* biofilms on the membranes were developed for 24 h at ~40 psi at 27 °C in recirculation cross flow without any filtration. The feed solution was removed, the system was flushed with 4 L of fresh M9G medium, and centrifuged (3,750 × *g* for 10 min at 4 °C) *P. aeruginosa* PAO1 cells from overnight cultures were added to another freshly prepared 4 L of M9G with 300 μg/mL Cm and 250 μg/mL Cb supplemented with 15 mM L-arginine and 1.6% L-arabinose at an initial turbidity of 0.002 or 0.01. The challenge experiment continued for ~72–96 h (depending on system stability) at ~200 psi at 27 °C with collection of flux data. After the completion of the experiments, the membranes were collected in 0.85% sterile NaCl solution, and immediate confocal microscopy analysis was performed on different sections of the membrane.

EH Removal via Once-Through Membrane Treatment. *E. coli* TG1/pBdcAE50Q-*lasI-lasR*/pBNos-*echA* and control (*E. coli* TG1/pBdcAE50Q-*lasI-lasR*/pBNos) biofilms were grown on NF90 membranes using M9G supplemented with 15 mM L-arginine (substrate for NOS) and 1.6% L-arabinose (inducer of *bNos* and *echA*) under static conditions for 24 h. The medium was removed from the stirred cell, and the biofilm was challenged with 10 mM epichlorohydrin in 5 mM NaCl solution with the pH adjusted to 9 (44) to maintain a constant pH throughout the experiment and analysis, thus minimizing unwanted dissociation. After incubation for 5 min, the membrane system was pressurized to 50 psi via N₂, permeate samples were collected at 10–20 min and at 20–30 min, and 100-μL samples were used for the EH assay.

ACKNOWLEDGMENTS. We thank Prof. Evgeny Nudler for providing the pBNos plasmid; Prof. Sharon Walker for *S. wittichii* RW1; Prof. Jintae Lee for his suggestions regarding confocal microscope experiments and COMSTAT analysis; Mark Signs of the Pennsylvania State Shared Fermentation Facility for help with the membrane system; and Fabiola Agramonte for conducting image analysis and assisting with experiments. This work was supported by National Science Foundation Grant CBET-1402063. T.K.W. is the Biotechnology Endowed Professor at the Pennsylvania State University.

- Gleick PH, et al. (2014) *The World's Water: The Biennial Report on Freshwater Resources* (Island Press, Washington, DC), Vol 8.
- Baroni L, Cenci L, Tettamanti M, Berati M (2007) Evaluating the environmental impact of various dietary patterns combined with different food production systems. *Eur J Clin Nutr* 61(2):279–286.
- Shannon MA, et al. (2008) Science and technology for water purification in the coming decades. *Nature* 452(7185):301–310.
- Greenlee LF, Lawler DF, Freeman BD, Marrot B, Moulin P (2009) Reverse osmosis desalination: Water sources, technology, and today's challenges. *Water Res* 43(9):2317–2348.
- Barnes RJ, et al. (2013) Optimal dosing regimen of nitric oxide donor compounds for the reduction of *Pseudomonas aeruginosa* biofilm and isolates from wastewater membranes. *Biofouling* 29(2):203–212.
- Elimelech M, Phillip WA (2011) The future of seawater desalination: Energy, technology, and the environment. *Science* 333(6043):712–717.
- Mansouri J, Harrison S, Chen V (2010) Strategies for controlling biofouling in membrane filtration systems: Challenges and opportunities. *J Mater Chem* 20(22):4567–4586.
- Matin A, Khan Z, Zaidi SMJ, Boyce MC (2011) Biofouling in reverse osmosis membranes for seawater desalination: Phenomena and prevention. *Desalination* 281:1–16.
- Herzberg M, Elimelech M (2007) Biofouling of reverse osmosis membranes: Role of biofilm-enhanced osmotic pressure. *J Membr Sci* 295(1–2):11–20.
- Vrouwenvelder JS, Graf von der Schulenburg DA, Kruithof JC, Johns ML, van Loosdrecht MCM (2009) Biofouling of spiral-wound nanofiltration and reverse osmosis membranes: A feed spacer problem. *Water Res* 43(3):583–594.
- Vrouwenvelder JS, van der Kooij D (2001) Diagnosis, prediction and prevention of biofouling of NF and RO membranes. *Desalination* 139(1–3):65–71.
- Al Ashhab A, Herzberg M, Gillor O (2014) Biofouling of reverse-osmosis membranes during tertiary wastewater desalination: Microbial community composition. *Water Res* 50:341–349.
- Al Ashhab A, Gillor O, Herzberg M (2014) Biofouling of reverse-osmosis membranes under different shear rates during tertiary wastewater desalination: Microbial community composition. *Water Res* 67:86–95.
- Bereschenko LA, Stams AJM, Euverink GJW, van Loosdrecht MCM (2010) Biofilm formation on reverse osmosis membranes is initiated and dominated by *Sphingomonas* spp. *Appl Environ Microbiol* 76(8):2623–2632.
- Ghayeni SBS, Beatson PJ, Schneider RP, Fane AG (1998) Adhesion of waste water bacteria to reverse osmosis membranes. *J Membr Sci* 138(1):29–42.
- Barnes RJ, et al. (2015) Nitric oxide treatment for the control of reverse osmosis membrane biofouling. *Appl Environ Microbiol* 81(7):2515–2524.
- Kim SR, et al. (2013) Biofouling control with bead-entrapped quorum quenching bacteria in membrane bioreactors: Physical and biological effects. *Environ Sci Technol* 47(2):836–842.
- Siddiqui MF, Sakinah M, Singh L, Zularisam AW (2012) Targeting N-acyl-homoserine-lactones to mitigate membrane biofouling based on quorum sensing using a bio-fouling reducer. *J Biotechnol* 161(3):190–197.
- Miller DJ, et al. (2012) Short-term adhesion and long-term biofouling testing of polydopamine and poly(ethylene glycol) surface modifications of membranes and feed spacers for biofouling control. *Water Res* 46(12):3737–3753.
- Kochkodan V, Hilal N (2015) A comprehensive review on surface modified polymer membranes for biofouling mitigation. *Desalination* 356:187–207.
- Yang HL, Lin JCT, Huang C (2009) Application of nanosilver surface modification to RO membrane and spacer for mitigating biofouling in seawater desalination. *Water Res* 43(15):3777–3786.
- Hong SH, et al. (2012) Synthetic quorum-sensing circuit to control consortial biofilm formation and dispersal in a microfluidic device. *Nat Commun* 3:613.
- Williams P, Cámara M (2009) Quorum sensing and environmental adaptation in *Pseudomonas aeruginosa*: A tale of regulatory networks and multifunctional signal molecules. *Curr Opin Microbiol* 12(2):182–191.
- Kaplan JB (2010) Biofilm dispersal: Mechanisms, clinical implications, and potential therapeutic uses. *J Dent Res* 89(3):205–218.
- Davies DG, Marques CNH (2009) A fatty acid messenger is responsible for inducing dispersion in microbial biofilms. *J Bacteriol* 191(5):1393–1403.
- Barraud N, et al. (2009) Nitric oxide-mediated dispersal in single- and multi-species biofilms of clinically and industrially relevant microorganisms. *Microb Biotechnol* 2(3):370–378.
- Nakhmachik A, Wilde C, Rowe-Magnus DA (2008) Cyclic-di-GMP regulates extracellular polysaccharide production, biofilm formation, and rugose colony development by *Vibrio vulnificus*. *Appl Environ Microbiol* 74(13):4199–4209.
- Yu S, et al. (2015) PslG, a self-produced glycosyl hydrolase, triggers biofilm disassembly by disrupting exopolysaccharide matrix. *Cell Res* 25(12):1352–1367.
- Li Y, et al. (2014) BdlA, DipA and induced dispersion contribute to acute virulence and chronic persistence of *Pseudomonas aeruginosa*. *PLoS Pathog* 10(6):e1004168.
- Kulasakara H, et al. (2006) Analysis of *Pseudomonas aeruginosa* diguanylate cyclases and phosphodiesterases reveals a role for bis-(3'-5')-cyclic-GMP in virulence. *Proc Natl Acad Sci USA* 103(8):2839–2844.
- Lee VT, et al. (2007) A cyclic-di-GMP receptor required for bacterial exopolysaccharide production. *Mol Microbiol* 65(6):1474–1484.
- Barraud N, et al. (2009) Nitric oxide signaling in *Pseudomonas aeruginosa* biofilms mediates phosphodiesterase activity, decreased cyclic di-GMP levels, and enhanced dispersal. *J Bacteriol* 191(23):7333–7342.
- Gusarov I, et al. (2008) Bacterial nitric-oxide synthases operate without a dedicated redox partner. *J Biol Chem* 283(19):13140–13147.
- Römling U, Galperin MY, Gomelsky M (2013) Cyclic di-GMP: The first 25 years of a universal bacterial second messenger. *Microbiol Mol Biol Rev* 77(1):1–52.
- Rossi AM, Migliore L, Loprieno N, Romano M, Salmons M (1983) Evaluation of epichlorohydrin (ECH) genotoxicity. Microsomal epoxide hydrolase-dependent deactivation of ECH mutagenicity in *Schizosaccharomyces pombe* in vitro. *Mutat Res* 109(1):41–52.
- US Environmental Protection Agency (2016) Drinking water contaminants—Standards and regulations. Available at <https://www.epa.gov/dwstandardsregulations>. Accessed April 22, 2016.
- WHO (2016) Epichlorohydrin in drinking water. Available at www.who.int/water_sanitation_health/dwaq/chemicals/epichlorohydrin.pdf. Accessed April 22, 2016.
- Pesci EC, Pearson JP, Seed PC, Iglewski BH (1997) Regulation of *las* and *rhl* quorum sensing in *Pseudomonas aeruginosa*. *J Bacteriol* 179(10):3127–3132.
- Ma Q, Yang Z, Pu M, Peti W, Wood TK (2011) Engineering a novel c-di-GMP-binding protein for biofilm dispersal. *Environ Microbiol* 13(3):631–642.
- Barnes RJ, et al. (2014) The roles of *Pseudomonas aeruginosa* extracellular polysaccharides in biofouling of reverse osmosis membranes and nitric oxide induced dispersal. *J Membr Sci* 466:161–172.
- Gutman J, Herzberg M, Walker SL (2014) Biofouling of reverse osmosis membranes: Positively contributing factors of Sphingomonas. *Environ Sci Technol* 48(23):13941–13950.
- Krijgheld KR, Vandergen A (1986) Assessment of the impact of the emission of certain organochlorine compounds on the aquatic environment. 3. Epichlorohydrin. *Chemosphere* 15(7):881–893.
- Jacobs MJH, Van den Wijngaard AJ, Pentenga M, Janssen DB (1991) Characterization of the epoxide hydrolase from an epichlorohydrin-degrading *Pseudomonas* sp. *Eur J Biochem* 202(3):1217–1222.
- Rui L, Cao L, Chen W, Reardon KF, Wood TK (2004) Active site engineering of the epoxide hydrolase from *Agrobacterium radiobacter* AD1 to enhance aerobic mineralization of *cis*-1,2-dichloroethylene in cells expressing an evolved toluene ortho-monooxygenase. *J Biol Chem* 279(45):46810–46817.
- Steinle-Darling E, Zedda M, Plumlee MH, Ridgway HF, Reinhard M (2007) Evaluating the impacts of membrane type, coating, fouling, chemical properties and water chemistry on reverse osmosis rejection of seven nitrosoalkylamines, including NDMA. *Water Res* 41(17):3959–3967.
- Zenker MJ, Borden RC, Barlaz MA (2003) Occurrence and treatment of 1,4-dioxane in aqueous environments. *Environ Eng Sci* 20(5):423–432.
- Plumlee MH, López-Mesas M, Heidlberger A, Ishida KP, Reinhard M (2008) N-nitrosodimethylamine (NDMA) removal by reverse osmosis and UV treatment and analysis via LC-MS/MS. *Water Res* 42(1–2):347–355.
- Molin S, et al. (1987) Conditional suicide system for containment of bacteria and plasmids. *Biotechnology* 5:1315–1318.
- Becht NO, Malik DJ, Tarleton ES (2008) Evaluation and comparison of protein ultra-filtration test results: Dead-end stirred cell compared with a cross-flow system. *Separ Purif Tech* 62(1):228–239.
- Krieg HM, Modise SJ, Keizer K, Neomagus HWJP (2004) Salt rejection in nanofiltration for single and binary salt mixtures in view of sulphate removal. *Desalination* 171(2):205–215.
- Donlan RM (2002) Biofilms: Microbial life on surfaces. *Emerg Infect Dis* 8(9):881–890.
- Fraser DW, et al. (1977) Legionnaires' disease: Description of an epidemic of pneumonia. *N Engl J Med* 297(22):1189–1197.
- Best M, et al. (1983) Legionellaceae in the hospital water-supply. Epidemiological link with disease and evaluation of a method for control of nosocomial legionnaires' disease and Pittsburgh pneumonia. *Lancet* 2(8345):307–310.
- Nickel JC, Ruseska I, Wright JB, Costerton JW (1985) Tobramycin resistance of *Pseudomonas aeruginosa* cells growing as a biofilm on urinary catheter material. *Antimicrob Agents Chemother* 27(4):619–624.
- Douglas LJ (2003) Candida biofilms and their role in infection. *Trends Microbiol* 11(1):30–36.
- Costerton JW, Stewart PS, Greenberg EP (1999) Bacterial biofilms: A common cause of persistent infections. *Science* 284(5418):1318–1322.
- Singh PK, et al. (2000) Quorum-sensing signals indicate that cystic fibrosis lungs are infected with bacterial biofilms. *Nature* 407(6805):762–764.
- Hyde JAJ, Darouiche RO, Costerton JW (1998) Strategies for prophylaxis against prosthetic valve endocarditis: A review article. *J Heart Valve Dis* 7(3):316–326.
- Sbordone L, Bortolaia C (2003) Oral microbial biofilms and plaque-related diseases: Microbial communities and their role in the shift from oral health to disease. *Clin Oral Invest* 7(4):181–188.
- Cryer J, Schipor I, Perloff JR, Palmer JN (2004) Evidence of bacterial biofilms in human chronic sinusitis. *ORL J Otorhinolaryngol Relat Spec* 66(3):155–158.
- Malfertheiner P, Link A, Selgrad M (2014) *Helicobacter pylori*: Perspectives and time trends. *Nat Rev Gastroenterol Hepatol* 11(10):628–638.
- Yonezawa H, et al. (2013) Impact of *Helicobacter pylori* biofilm formation on clarithromycin susceptibility and generation of resistance mutations. *PLoS One* 8(9):e73301.
- Sambrook JF, Russell DW (2001) *Molecular Cloning: A Laboratory Manual* (Cold Spring Harbor Lab Press, New York), 3rd Ed.
- Sambrook J, Fritsch EF, Maniatis T (1989) *Molecular Cloning, A Laboratory Manual* (Cold Spring Harbor Lab Press, Cold Spring Harbor, NY), 2nd Ed.
- Fletcher M (1977) The effects of culture concentration and age, time, and temperature on bacterial attachment to polystyrene. *Can J Microbiol* 23(1):1–6.

66. Heydorn A, et al. (2000) Quantification of biofilm structures by the novel computer program COMSTAT. *Microbiology* 146(Pt 10):2395–2407.
67. Rink R, Fennema M, Smids M, Dehmel U, Janssen DB (1997) Primary structure and catalytic mechanism of the epoxide hydrolase from *Agrobacterium radiobacter* AD1. *J Biol Chem* 272(23):14650–14657.
68. Leungsakul T, Johnson GR, Wood TK (2006) Protein engineering of the 4-methyl-5-nitrocatechol monooxygenase from *Burkholderia* sp. strain DNT for enhanced degradation of nitroaromatics. *Appl Environ Microbiol* 72(6):3933–3939.
69. Boerlage SFE, Kennedy MD, Dickson MR, El-Hodali DEY, Schippers JC (2002) The modified fouling index using ultrafiltration membranes (MFI-UF): Characterisation, filtration mechanisms and proposed reference membrane. *J Membr Sci* 197(1-2): 1–21.
70. Jacobs MA, et al. (2003) Comprehensive transposon mutant library of *Pseudomonas aeruginosa*. *Proc Natl Acad Sci USA* 100(24):14339–14344.
71. Davies DG, et al. (1998) The involvement of cell-to-cell signals in the development of a bacterial biofilm. *Science* 280(5361):295–298.